Effect of Working Fluids in Thermodynamic Performance Analysis of Organic Rankine Cycle

[1]SUJIT KUMAR,
Gandhi Institute of Excellent Technocrats, Bhubaneswar, India
[2]TUSHAR TAPAN SAHOO,
Krupajal Group of Institutions, Bhubaneswar, Odisha, India

Abstract
Working fluids play a crucial part in Organic Rankine Cycle (ORC) which is able to recover the low-grade heat from renewable or waste heat sources. Current work focuses on establishing the relationship between ORC performance parameters (First law efficiency, Second law efficiency, Turbine Size Factor (TSF), Net Work Output) and the source temperature, Turbine inlet Temperature, PPTD and turbine efficiency by employing 4 different working fluids (RC318, R600a, R32, R134a). The working fluids are so chosen that two are dry fluids (RC318, R600a) having higher critical temperatures and two are wet fluids (R143a, R32) with comparatively lower critical temperatures. An EES program has been developed to analyze these performance parameters with varied input conditions. The cycle efficiency increases monotonically with rising HST, TIT and turbine efficiency. On the contrary, TSF decreases with increasing HST, TIT and turbine efficiency.Net Work Output increases with increasing HST, TIT and Turbine Efficiency but decreases with increasing PPTD.
Keywords: *ORC, RC, First law efficiency, Second law efficiency, TSF, Net Work output, HST.*

1. Introduction

The world's current development is largely due to the increasingly efficient and extensive usage of numerous forms of energy. The surge in global energy consumption in the last few decades has shown that fossil fuel energy sources alone will not be able to meet future energy demands.
As fossil fuel consumption rises, more and more industrial activities create waste heat. Industrial waste heat is energy that is generated as a result of industrial processes but is not used. According to several studies, the precise amount of industrial waste heat is poorly recorded; it is estimated that 25 to 55 % of the input energy in enterprises is really used, while the rest is discharged [1]. While it is nearly difficult to mitigate industrial waste heat losses, several facilities and heat recovery technologies can be put in place to reduce waste heat by enhancing equipment efficiency and energy use. Energy extraction from superheated steam, turbine exhaust, solar energy, and biomass energy becomes a typical method for most industries to generate alternative energy. Low-grade heat inputs can be turned into electrical energy by means of an ORC (Organic Rankine Cycle) system. The ORCs' core concepts are quite similar to those of the traditional Rankine cycle. The ORC, on the other hand, employs an organic working fluid that has a high vapor pressure and lowers boiling point than water. Compared with the conventional Rankine cycle, these features of organic fluids significantly improve ORC cycle efficiency [2]. To generate useful work from these low-grade heat sources, efficient and effective solutions must be developed. An ORC is an appropriate tool for accomplishing this goal. The ORC uses an organic working fluid with a large molecular mass and a phase change of liquid to vapour that occurs at a lower temperature than the phase change of water to steam at the same pressure. Organic fluids can be used to recover heat from low-grade sources [3].
ORCs usage organic working fluids, which are daintier than water in the context of using a low-temperature heat source. Unlike traditional steam cycles, the ORC cycle is an appealing benchmark for local and small-scale power generation.
In 1883, Frank W. Ofledt patented the naphtha engine, which serves the same purpose as the ORC. To replace the steam engine on the boat, naphtha was utilized as the working fluid instead of water [4].
Harry Zvi designed the very first model of the ORC development in the early 1960s [5]. This model was primarily secondhand to recover low-grade heat, like how solar energy is recycled to convert low-temperature sources to electricity. Harry Zvi also invented a turbine that could work and operate at a relatively low temperature. An Israeli corporation later privatized this innovation in 1965[6].
ORC installations are currently successful in a number of nations. Various countries nowadays are utilizing

waste heat with ORCs. The majority of ORC systems are found in Germany, Italy, Canada, and the United States, while Belgium, Austria, Romania, Russia, Finland, Swaziland, Morocco, and India have only one unit [7]. The gas, glass, and cement industries are the most common businesses that employ the ORC system to recover waste heat in different nations. Chang et al. analyzed the combined generationof heat and power using an ORC to enhance the utilization of energy and reduce carbon emission [8]. Karellas and Braimakis analyzed solar (using PTC)-biomass energy powered ORC integrated VCRS system with R134a, R152a, R245fa working fluids in the system [9]. Rostamzadeh et al. investigated the performance of solar energy powered ORC integrated ejector refrigeration cycle and reported R123/isobutene as most appropriate fluid pair among R123, R245fa, and isobutane ORC working fluids [10]. Amirante et al. performed energetic and economic analysis of biomass- based hybrid system which comprises commercially available 280 kW organic Rankine cycle unit and absorption chiller for air conditioning of airport buildings. The payback duration and internal rate of return, according to the research, are 6 years and 21%, respectively [11].

Vazhappilly et al. used a combined biomass-solar energy source for ORC integrated compression unit for microscale applications. The system is analyzed with R134a, R152a and R245fa working fluids and reported 7 years payback period [12]. Jradi and Riffat experimentally investigated a micro-scale biomass-based hybrid system using a liquid desiccant cooling system and reported overall efficiency of 83% for combined heat and power mode and 85% for regenerations [13]. Akramiet al. carried out energetic and Exergo- economic assessment of the geothermal ORC integrated absorption cycle and reported 35% energy efficiency and 49% exergy efficiency [14]. Arora et al. conducted an experiment on Vapour Compression Refrigeration (VCR) cycle to find the COP, exergy destruction as well as exergetic efficiency of working fluid R-22, R-407C and R-410A. Outcomes of experimentation work show that COP was greater for R22 [15]. Kalla et al. carried out the performance analysis using various kinds of working fluids i.e. R22, R407C, R432A, R438A and NM1 (R32/R125/R600a). The results indicate that the higher COP was calculated for R-22 in the operating temperature range of 45-50°C [16]. Agrawal et al. studied the exergy analysis of VCR cycle employing the three different working fluids (HFO-R1234ze, R1234yf, & HFC-R134a) and a computer programme also built up in EES for carrying out the performance in the term of COP, and exergy efficiency [17]. Agrawal et al. performed the experimental analysis using different working fluids (R134a, R-1234Ze, and R1243yf). The result shows that the COP of R-1234Ze was 1.87% higher than reaming twoworking fluids [18].

3. Mathematical Modeling

It is required to implement Physical model in a mathematical model to aid in the analysis of engineering problems. To execute this, we first build state point equations for thermodynamic characteristics and then, using software or directly from the reference, develop a polynomial for thermodynamic properties.

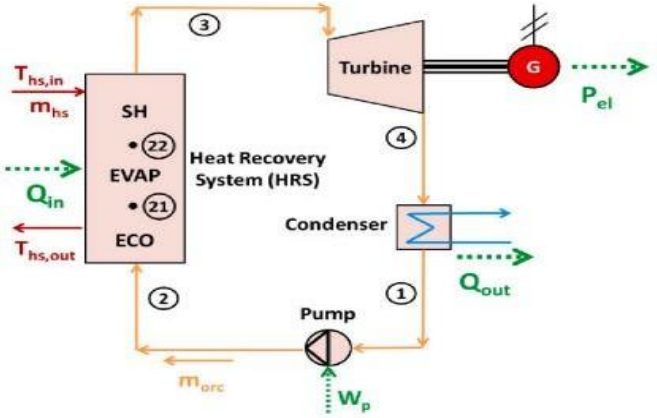

Fig. 1: Schematic of the organic Rankine cycleThe assumptions considered for this study are

(1) Steady-state operating conditions are considered.(2 Pressure drop and heat losses are neglected.

(3) Kinetic energy and potential energy changes are neglected.

(4) WFs come out as saturated fluids from the evaporator and condenser.

Mass balance:

$$\sum in\ \dot{m} = \sum out\ m \quad (1)$$

Energy balance:

$$Q - W = \sum out\ \dot{m}\ h - \sum in\ \dot{m} h \quad (2)$$

Net power output of ORC system (W_{net}) is computed using Eq.

$$W_{net} = W_{turbine} - W_{pump} \quad (3)$$

$$W_{pump} = \frac{m(h_{4s} - h_3)}{\eta_{pump}} \quad (4)$$

$$W_{turbi} = (h_1 - h_{2s})m \times \eta_{Turbine} \quad (5)$$

I[st] and II[nd] law efficiencies of the ORC (η_I and η_{II}) are evaluated using Eq.

$$\eta_I = \frac{W_{net}}{Q_{in}} \quad (6)$$

$$\eta_{II} = \frac{W_{net}}{[Q_{in}(1 - T_o)/T_m]} \quad (7)$$

Turbine size factor (TSF) is directly proportional to actual turbine size and is evaluated using Eq.

$$TSF = \frac{\sqrt{\Delta H_{is}}}{V_2} \quad (8)$$

Where h_1= Specific enthalpy at turbine entry, h_{2s}=Specific enthalpy at turbine exist, h_3=specific enthalpy at pump entry, h_{4s}=Specific enthalpy at pump exist,
V_2=volume flow rate of WF inside the turbine.

4. Result and Discussion

In this research, a thermodynamic model was created using Engineering Equation Solver software, and the findings of the researchare presented in the sections below.
The input conditions that were considered in the study are listed below.

Input Parameters	Value
Condenser temperature ($T_{condensor}$)	28°C
Evaporator temperature ($T_{evaporator}$)	120°C
Turbine and evaporator isentropic efficiency	0.9
Mass flow rate of heat source fluid	1.2kg/s

Influence of Heat Source Temperature

The Ist law and IInd law efficiency as well as TSF of ORC has been analyzed employing R32, R600a, R134a, and RC318 such as working fluid using parametric analysis. To predict the thermodynamic performance of ORC with varied heat source temperatures, a computer model in Engineering Equation Solver (EES) was built.

Influence of heat source temperature in ORC's I^{st} law effectiveness is shown in Figure1. A similar trend is found in the variation of Ist law efficiency for all the four WFs. It demonstrates a monotonic increase of Fist law efficiency with rising heat source temperature. I^{st} law efficiencies increased 40.12% for R32, 74.49% for R600a, 58.85% for R134a, and 59.70 % for RC318 as TIT rises from 100 to 145 ℃ with a step of 50C. The best thermal efficiency is achieved by RC318; it is followed by R32, R600a, and R134a.

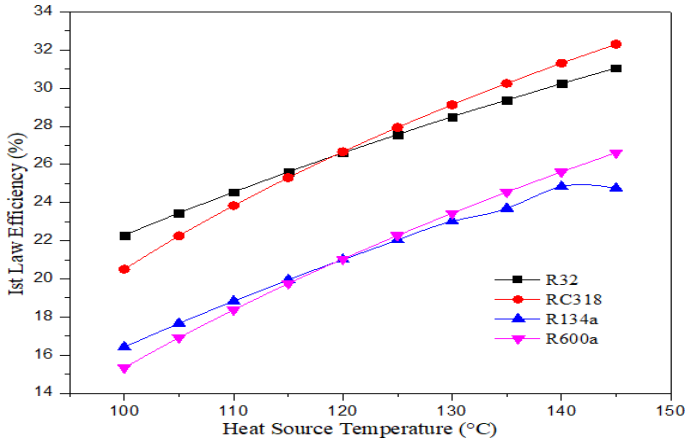

Fig.2: Variation First law efficiency w.r.t HST

Fig. 3 depicts IInd law efficiency as a function of HST. It demonstrates a monotonic increase in IInd law efficiency for all the WFsin consideration, with increasing heat source temperature. The IInd law efficiencies increased 40.01% for R32, 75.44 % for R600a,

58.55 % for R134a, and 59.52% for RC318 as TIT rises from 100 to 145 ℃ with a step of 5^0C. The best thermal efficiency isachieved by RC318; it is followed by R32, R600a, and R134a.

The reason is that as the mean temperature of heat addition increases the cycle irreversibility decreases which in turn increases thecycle efficiency.

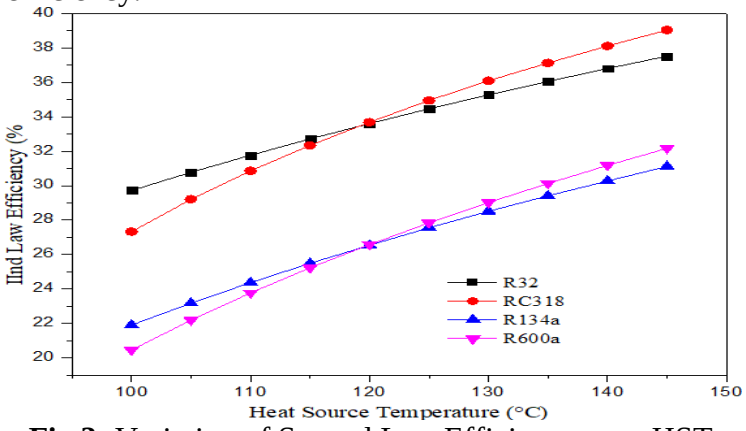

Fig.3: Variation of Second Law Efficiency w.r.t HST

Fig.4 demonstrates TSF as a function of HST. With heat source getting bigger, TSF gets smaller. Small size factors are achieved for R32 at maximum HSTs for the conditions under consideration. Because of low evaporation pressure, R600a needs the greatest size parameter. At all of the HSTs, R32 has the smallest turbine size parameter.

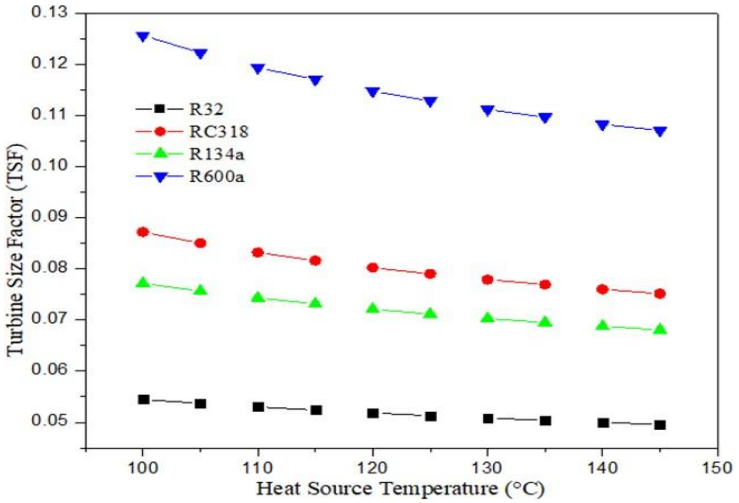

Fig.4: Variation of TSF w.r.t HST

Fig.6 depicts Net Work Output as a function of HST. For the HST range of 100 to 145^{0}C, the Net Work Output increases gradually. For this case R32 has the highest Net Work output over all the temperature range of heat source followed by RC318, R600a and R134a.R134a shows the least Net Work output overall HST range. But the increase is not so significant. This is because with increase in HST the mean temperature of heat addition increases which in turn increases the available energy and as a result Net Work Output increases.

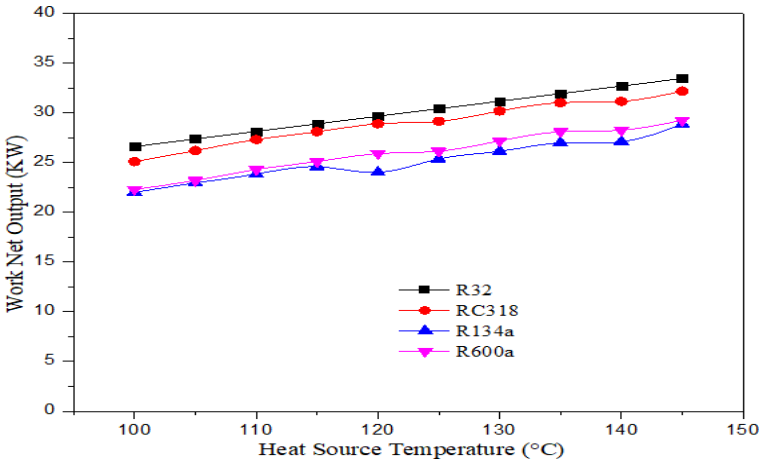

Fig.5: Variation of Net Work Output with HST

Effect of Turbine Inlet Temperature

The objective of this research is to examine Ist law, IInd law efficiency, as well as TSF of ORC employing R32, R600a, R134a, andRC318 such as working fluid using parametric analysis. To predict thermodynamic analysis of fried working fluid at various TIT,a computer programme in EES was constructed.

Influence of turbine inlet temperature on ORC first law efficiency is shown in Fig. 5. The effects of heat source temperature on first law efficiency are found to be similar for different working fluids. It demonstrates that when the turbine input temperature rises, the very first law thermal efficiency grows monotonically. 1st law efficiencies for R32, R600a, R134a, and RC318 improve approximately as TIT rises from 100 to 370 ℃. The best thermal efficiency is achieved by RC318; it is followed by R32, R600a, and R134a, which all perform poorly.

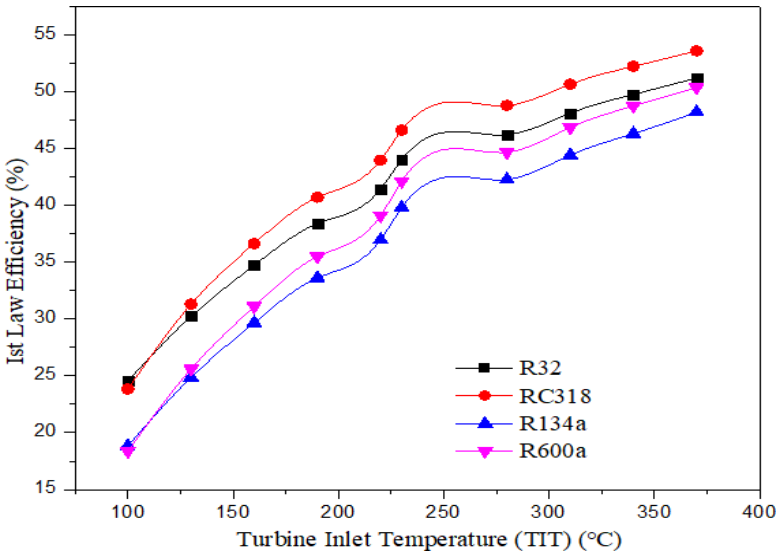

Fig.6: Variation of First-law efficiency w.r.t TIT

Fig.7 displays variability of II[nd] law efficiency versus turbine inlet temperature. II[nd] law efficiency improves as turbine input temperature rises. The II[nd] law efficiencies for R32, R600a, R134a, and RC318 increase approximately as turbine inlet temperature rises from 100 to 370 °C. The best thermal efficiency is achieved by RC318; it is followed by R32, R600a, and R134a, which all perform poorly. The impacts of TIT on the ORC's turbine size factor are seen in Fig. 7. When the TIT is increased, the TSF generally drops. R32 has tiny size factors at high TITs for conditions under consideration. Because of the low evaporation pressure, R600a requires the biggest size parameter. R32 has the smallest turbine size parameter across all TITs.

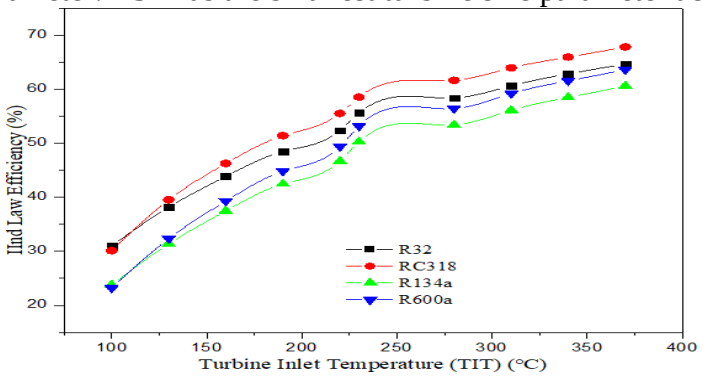

Fig. 7: Variation of second law efficiency w.r.t TIT

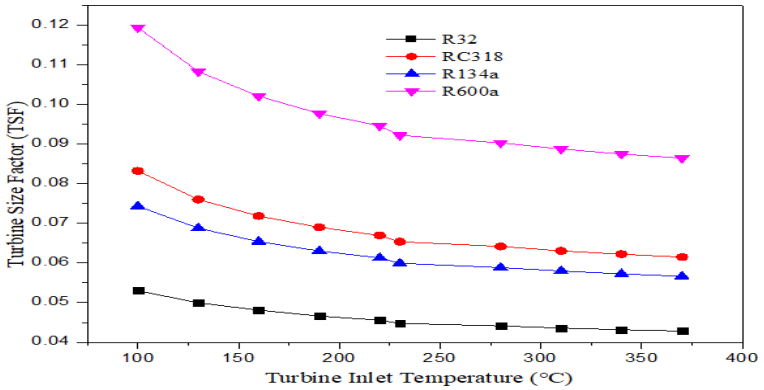

Fig.8: Variation of TSF w.r.t TIT

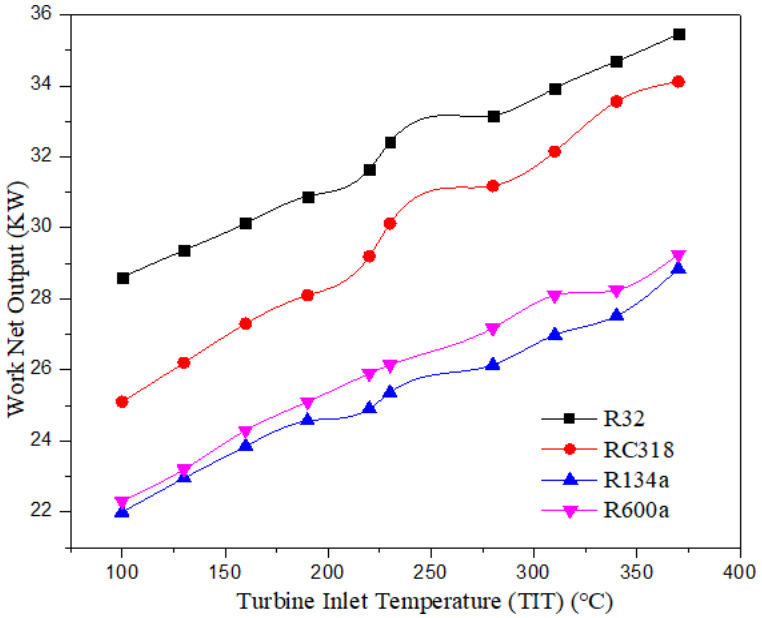

Fig.9: Variation of Net Work Output w.r.t TIT

Fig.9 depicts Net Work Output as a function of TIT. It can be inferred from the graph that for the TIT varying from 100 to 370^{0}C with a step increase of 30^{0}C, Net Work Output increases for all the four WFs. R32 achieves the highest Net Work Output over the range of TITs while RC318, R600a, R134a trail behind it. R134a has the minimum Net Work Output over all the range of Turbine Inlet Temperature.

Influence of Pinch Point Temperature Variance

Aim of the current study is to examine 1st law efficiency, IInd law efficiency, as well as TSF of ORC employing R32, R600a, R134a, and RC318. To predict thermodynamic analysis of used working fluid with varied pinch point temperature differences, a computer programme in EES was constructed. Influence of pinch point temperature difference on ORC first law efficiency is shown in Figure9. Effects of PPTD on 1st law efficiency are shown to be the same manner for different working fluids. Ist law thermal efficiency diminishes monotonically as pinch point temperature difference increases. Ist law efficiencies for R32, R600a, R134a, and RC318 decline as PPDT rises from 10 to 28 ℃. R32 has the maximum thermal efficiency, followed by RC318, R134a, and R600a.

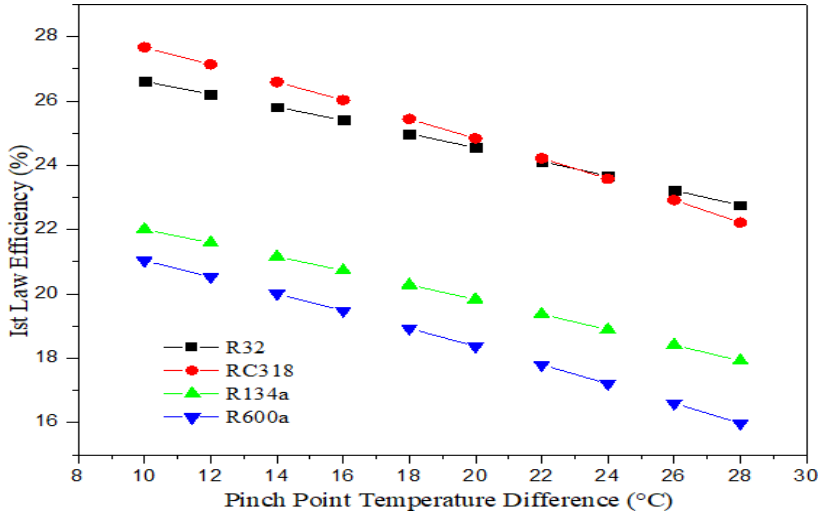

Fig. 10: Variation of First Law Efficiency w.r.t PPTD

The impact of pinch point temperature difference on ORC second law efficiency is shown in Fig.10. The effect of pinch point temperature differential on 1st law efficiency is shown to be the same manner for different working fluids. 1st law thermal efficiency diminishes monotonically as PPTD increases. 1st law efficiencies for R32, R600a, R134a, and RC318 decline as PPTD rises from 10 to 28 ℃. R32 has the maximum thermal efficiency, trailed by RC318, R134a, and R600a.

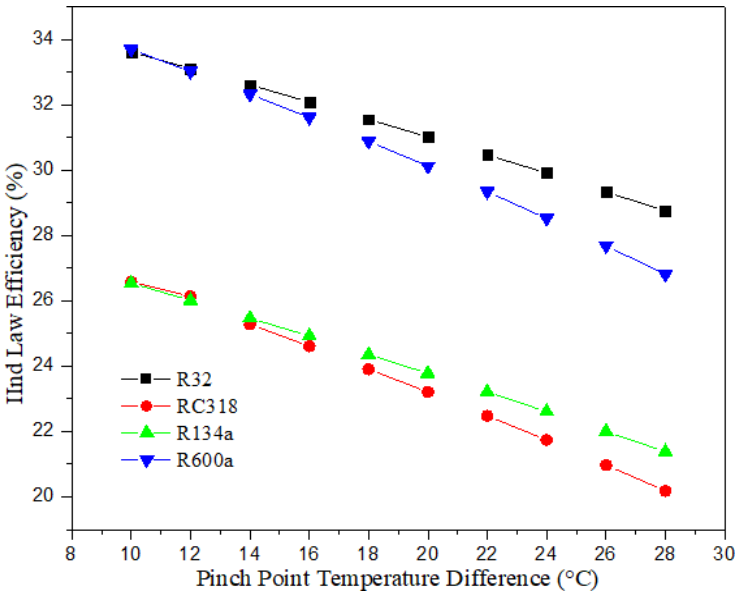

Fig.11: Variation of Second Law Efficiency w.r.t PPTD

Fig. 12 depicts TSF as a function of PPTD. The turbine size factor is always increasing when the TIT is increased. R32 has tiny size factors at high TITs for the conditions under consideration. Because of the low evaporation pressure, R600a requires the biggest size parameter. R32 has the smallest turbine size parameter across all TITs.

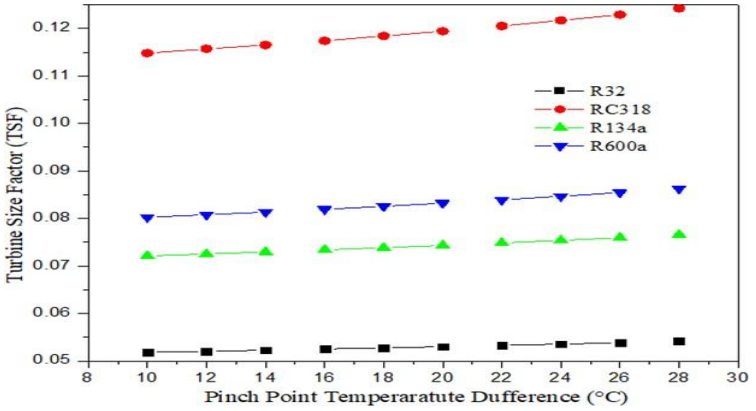

Fig.12: Variation of TSF w.r.t PPTD

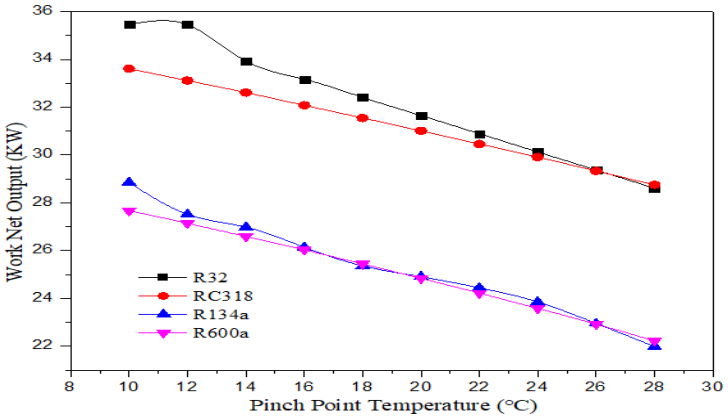

Fig.13: Variation of Net Work Output w.r.t PPTD

EFFECT OF TURBINE EFFICIENCY

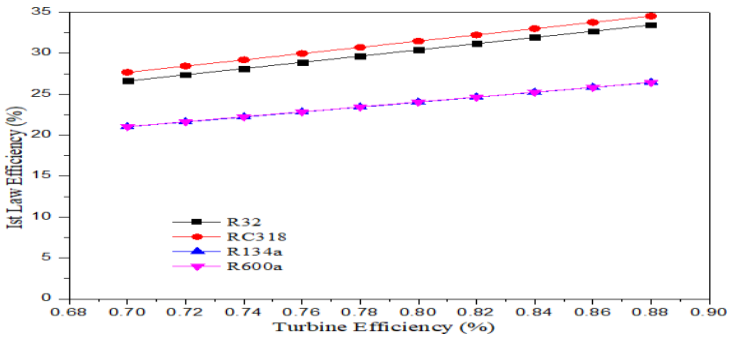

Fig.14: Variation of Ist law efficiency w.r.t Turbine efficiency

The influence of turbine efficiency on the ORC's first law efficiency is seen in Fig.13. The effects of turbine efficiency on first law efficiency are found to be consistent across different working fluids. It demonstrates that the first law thermal efficiency rises in lockstep with turbine efficiency. In a range of 70% to 88% turbine efficiencies with a step of 2%, the Ist law efficiency increases approximately for all the four WFs in consideration. Best Thermal efficiency is achieved by both RC318 and R32 outperforming R134a and R600a combined.

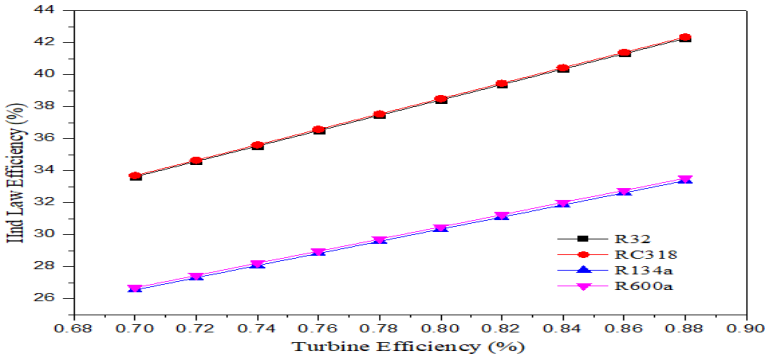

Fig.15: Variation Second Law Efficiency w.r.t turbine efficiency

Influence of turbine efficiency on the ORC's second law efficiency is illustrated in Fig.15. Effects of turbine efficiency on second law efficiency are found to be the same when using different operating fluids. It demonstrates that when turbine efficiency rises, the second law thermal efficiency rises in a monotonic fashion. As turbine efficiency rises from 70 percent to 80 percent the IInd law efficiency for all working fluids increases monotonically. The best thermal efficiency is achieved by R32 and RC318. R134a and R600a perform poorly.

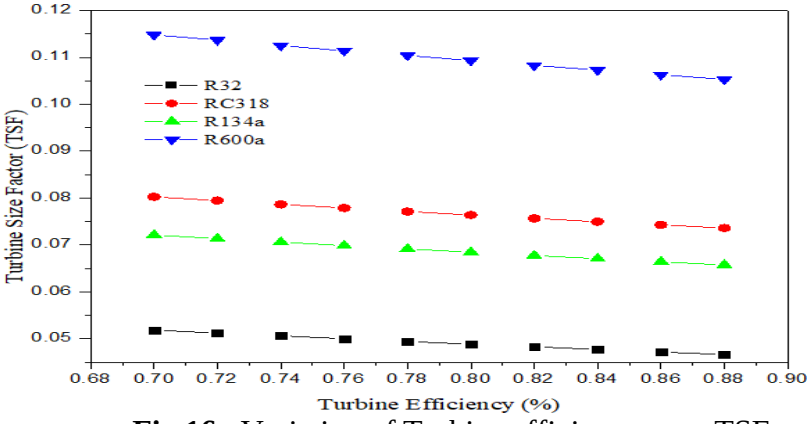

Fig.16: Variation of Turbine efficiency w.r.t TSF

Fig.16 depicts TSF as a function of Turbine efficiency. As the turbine Efficiency rises, TSF falls. Small size factor is achieved for higher turbine efficiency. As a result of low evaporation pressure, R600a requires the

greatest size parameter. At all turbine efficiencies, R32 reflects the smallest TSF.

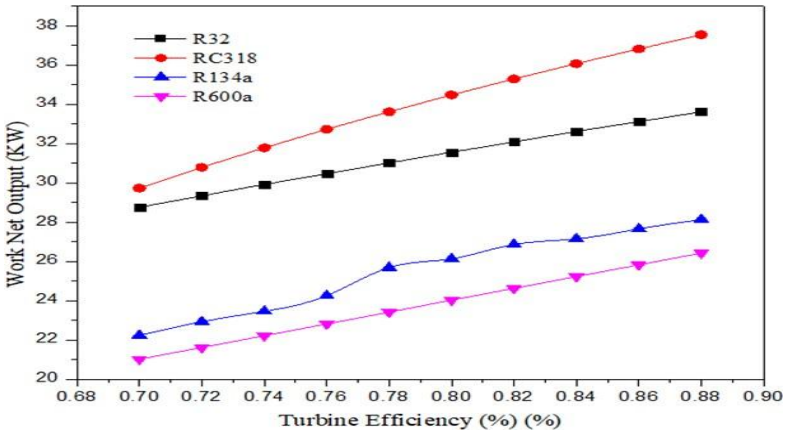

Fig.17: Variation of Net Work Output w.r.t Turbine Efficiency

Fig.17 depicts Net Work Output as a function of Turbine efficiency. It can be inferred that with increase in Turbine efficiency from 70 % to 88% with a step of 2%, Net Work Output increases gradually. Monotonic increase in Net Work outputs can be seen over the range of Turbine efficiency. RC318 reflects the highest Net Work Output value over the range of Turbine efficiency while R600a has the lowest one. R32 performs better than R134a, both being wet fluids

Conclusion

Thermodynamic efficiencies, Net Work Output and TSF of ORC employing R32, R600a, R134a, and RC318 as operating fluid are analyzed and compared. A simulation program in EES has is being designed to determine the thermodynamic performance of 4 different operational fluids with different TIT, PPTD, heat source, and turbine efficiency under constant external conditions.

- It is discovered in the current investigation that the effects of heat source temperature on I^{st} law and II^{nd} law efficiency were equivalent for all those working fluids used. With varying temperature of the source in the range of 100 - 145 ^{0}C with step of 5^0, the I^{st} and II^{nd} law efficiencies increases approximately considering all the WFs.
- TSF decreases with increase in the Temperature of heat source. At high TITs, R32 shows the smallest size factor. Because of the low evaporation pressure, R600a requires the biggest size parameter. Considering the range of TITs, R32 shows the minimum TSP.
- The effect of TIT on the I^{st} law and II^{nd} law efficiencies was found to be analogous while taking all the four working fluids into consideration. It reveals that when TIT rises, the first law and second law efficiencies increase monotonically. I^{st} and II^{nd} law efficiencies for R32, R600a, R134a, and RC318 increase precisely as TIT vary from 100 to 370°C. RC318 outperforms R32, R600a and R134a in terms of thermal efficiency.
- When the TIT is increased, the turbine size factor always drops. R32 has small size factors at high TITs for the conditions under consideration. Because of the low evaporation pressure, R600a requires the biggest size parameter. R32 has the smallest TSF considering all TITs in the range 100 to 370^0 with a step increase of 30^0C.
- The turbine size factor is always increasing when the TIT is increased. R32 has small size factors at high TITs for the conditions under consideration. Because of the low evaporation pressure, R600a requires the biggest size parameter. R32 realizes the smallest TSP considering all the WFs.
- Effects of turbine efficiency on I^{st} and II^{nd} law efficiencies were found to be alike while using WFs. It demonstrates that I^{st} law thermal efficiency rises unvaryingly as turbine efficiency increases. R32 and RC318 realize the best thermal efficiency while R134a and R600a realize lesser thermal efficiency.
- For the HST range of 100 to 145^0C the Net Work Output increases gradually. For this case R32 has the highest Net Work output over all the temperature ranges of the heat source followed by RC318, R600a and R134a.R134a shows the least Net Work Output over all the temperature ranges. But the increase is not so significant
- Net Work Output increases for all the four WFs. R32 achieves the highest Net Work Output over the range of TITs while RC318, R600a and R134a trail behind it. R134a has the minimum Net Work

Output over all the range of Turbine Inlet Temperature.

- Monotonic increase in Net Work outputs can be seen over the range of Turbine efficiency. RC318 reflects the highest Net Work Output value over the range of Turbine efficiency while R600a has the lowest one. R32 performs better than R134a, both being wet fluids.

Abbreviations

ORC	Organic Rankine Cycle
RC	Rankine Cycle
TIT	Turbine inlet
HS	TemperatureHeat
T	Source Temperature
TS	Turbine Size Factor
F	Turbine Size
TS	ParameterTurbine
P	Efficiency
TE	
VCC	Vapor Compression Cycle
PPTD	Pinch Point Temperature Difference
h	Enthalpy (kJ/kg.K)
$W_{turbine}$	Turbine Work
W_{pump}	Pump work
ηI	I^{st} law efficiency
ηII	II^{nd} law efficiency
ΔH_{is}	Isentropic Enthalpy
Q_{in}	differenceHeat Input

References

[1]. Virang H Oza, Nilesh M Bhatt, Optimization of Ammonia-Water Absorption Refrigeration System using Taguchi Method of Design of Experiment, International Journal of Mechanics and Solids, 13(2), 111-126, 2018.

[2]. K. S. AlQdah, "Performance and evaluation of aqua ammonia auto air conditioner system using exhaust waste energy",EnergyProcedia, vol. 6, 2011.

[3]. Satish Raghuvanshi, Govind Maheshwari, Analysis of Ammonia –Water (NH3-H2O) Vapor Absorption Refrigeration System based on First Law of Thermodynamics, International Journal of Scientific & Engineering Research, 2(8), 1-7, 2011.

[4]. Manzela, S. M. Hanriot, L. C. Gomez, and J. R. Sodre, "Using engine exhaust gas as an energy source for an absorption refrigeration system", Applied Energy, vol. 87, 2010.

[5]. Aman Shukla, C.O.P Derivation and Thermodynamic Calculation of Ammonia-Water Vapor Absorption Refrigeration System, International Journal of Mechanical Engineering and Technology, 6(5), 72-81, 2015.

[6]. J. Yadav and B. R. Singh, "Experimental set up of air conditioning system in automobile using exhaust energy", S-jpset, vol. 5, 2014.

[7]. Ahmed Ouadha, Youcef El-Gotni (2013), Integration of an ammonia-water absorption refrigeration system with a marine Diesel engine: A thermodynamic study, The 3rd International Conference on Sustainable Energy Information Technology, Procedia Computer

Science, 19, 754 – 761.

[8]. Huawei Chang, Zhongmin Wana Yao Zhenga Xi Chen, Shuiming Shu , Zhengkai TucdSiew ,Hw Chand "Energy analysis of a hybrid PEMFC–solar energy residential micro-CCHP system combined with an organic Rankine cycle and vapor compression cycle" Energy Conversion and Management, Volume 142, 15 June 2017, Pages 374-384.

[9]. Sotirios Karellas and Konstantinos Braimakis "Energy–exergy analysis and economic investigation of a cogeneration and tri-generation ORC–VCC hybrid system utilizing biomass fuel and solar power' Energy Conversion and Management, Volume 107, 1 January 2016, Pages 103-113

[10]. Hadi Rostamzadeh and Pejman Nouranib "Investigating potential benefits of a salinity gradient solar pond for ejector refrigeration cycle coupled with a thermoelectric generator" Energy, Volume 172, 1 April 2019, Pages 675-690

[11]. Riccardo Amirante ,Sergio Bruno, Elia Distaso, Massimo L, Scalab PaoloTamburrano. 'A biomass small-scale externally fired combined cycle plant for heat and power generation in rural communities" Renewable Energy Focus, Volume 28, March2019, Pages 36-46

[12]. C. V. Vazhappilly, T. Tharayil, A.P. Nagarajan, "Modeling and experimental analysis of generator in vapor absorption refrigeration system", Journal of Engineering Research and Application, vol. 3, no. 5, 2013.

[13]. M.Jradi and S.Riffat Experimental investigation of a biomass-fuelled micro-scale tri-generation system with an organic Rankine cycle and liquid desiccant cooling unit' Energy, Volume 71, 15 July 2014, Pages 80-93

[14]. Ehsan Akrami, Hossein Nami, , Faramarz, Ranjbar, "Hydrogen production using the waste heat of Benchmark pressurized Molten carbonate fuel cell system via combination of organic Rankine cycle and proton exchange membrane (PEM) electrolysis' Applied Thermal Engineering, Volume 114, 5 March 2017, Pages 631-638

[15]. Akhilesh Arora, B.B. Arora, B.D. Pathak and H.L. Sachdev. "Exergy analysis of a Vapour Compression Refrigeration system with R-22, R-407C and R-410A" Int. J. Exergy, Vol. 4, No. 4, 2007.

[16]. S.K. Kalla, B.B. Arora, J.A. Usmani "Performance Analysis of R22 and Its Substitutes in Air Conditioners" Journal of Thermal Engineering, Vol. 4, No. 1, pp. 1724-1736, January, 2018.

[17]. Shyam Agrawal, Akhilesh Arora, B.B.Arora "Exergy Analysis of Dedicated Mechanically Sub cooled Vapour Compression Refrigeration Cycle Using HFC-R134a, HFO-R1234ze and R1234yf" Part of the Lecture Notes in Civil Engineering book series (LNCE, volume 36)

[18]. Shyam Agarwal, Akhilesh Arora, B.B. Arora. "Energy And Exergy Investigations Of R1234yf And R1234ze As R134a Replacements In Mechanically Sub cooled Vapour Compression Refrigeration Cycle" Journal of Thermal Engineering, Vol. 7, No. 1, pp. 109-132, January, 2021